Multiple strategies for heat adaptation in rice endosperms revealed by on-site cell-specific analysis

Hiroshi Wada[1,†,*], Yuto Hatakeyama[1,†], Yayoi Onda[2], Hiroshi Nonami[2], Taiken Nakashima[3], Rosa Erra-Balsells[4], Satoshi Morita[1], Kenzo Hiraoka[5], Fukuyo Tanaka[6], and Hiroshi Nakano[1]

[1]Kyushu Okinawa Agricultural Research Center, National Agricultural Research Organization, Chikugo, Japan; [2]Graduate School of Agriculture, Ehime University, Matsuyama, Japan; [3]Faculty of Agriculture, Hokkaido University, Sapporo, Japan; [4]Department of Organic Chemistry, University of Buenos Aires, Buenos Aires, Argentina; [5]Clean Energy Research Center, The University of Yamanashi, Kofu, Japan; [6]Central Region Agricultural Research Center, National Agriculture and Food Research Organization, Tsukuba, Japan

[†]These authors contributed equally to this manuscript.

*For correspondence: hwada@affrc.go.jp

Abstract

Plant cells have multiple strategies to adapt to environmental stresses. Rice endosperms form chalkiness in a part of the tissue under heat conditions during the grain-filling stage, although nitrogen supply reduces chalky rice. Air spaces formed in the cells cause an irregular light reflection and create chalkiness, yet what exactly occurs remains unclear at cell level. Through on-site cell-specific analysis, we show that heat-treated cells adjust osmotically and retard protein synthesis to preserve protein storage vacuoles in the cytosol, resulting in air space formation. Application of nitrogen enhances heat tolerance to sustain protein body and amyloplast development during strong osmotic adjustment, which diminishes air spaces to avoid chalkiness. Hence, we conclude that rice endosperm cells could alter organelle compartments spatially during the heat adaptation, depending on the available nitrogen level. Our findings provide new insight into the cellular mechanism of rice chalky formation as a strategy for heat acclimation.

Introduction

Rice chalkiness is a critical trait that determines the rice quality (Hoshikawa, 1989). Currently, an increase in chalky rice induced by several environmental stresses, such as high temperature during the grain-filling stage, has been frequently observed under global

warming (Tashiro and Wardlaw, 1991a, 1991b; Morita et al., 2016). In chalky rice, air spaces formed in a part of endosperms among the loosely-packed starch granules causes significant random light reflection, thereby turning them into chalk (Tashiro and Wardlaw, 1991b). One of the major chalky rice, called 'white-back rice', frequently induced by exposure to high temperatures at the early ripening stage, exhibits chalkiness in the outer endosperms longitudinally aligned along the dorsal side of the kernels, where a greater abundance of protein bodies (PBs) are distributed than in the ventral side of the endosperm (Ellis et al., 1987; Hoshikawa, 1989). Moreover, white-back rice is known to be decreased by supplying nitrogen (N) prior to heat conditions (Perez et al., 1996; Wakamatsu et al., 2008). Since chalky formation occur only a part of endosperms, this phenomenon can be a cell-specific event. However, our current understanding of heat-induced rice chalkiness mostly relies on tissue analysis (e.g., Yamakawa et al., 2007); the underlying mechanism in cellular metabolism prior to the air space formation remains unclear. Moreover, the possible role of N during the heat response has not been spatially addressed at the metabolite level.

Storage proteins are major components that accumulate 5–8% in rice endosperms (Juliano, 1985; Hoshikawa, 1989). These proteins are typically stored into two types of protein bodies (PBs), called PBI and PBII (Tanaka et al., 1980; Herman and Larkins, 1999; Shewry and Halford, 2002; Onda, 2013). PBI is a small spherical granule of 1–2 μm in diameter with concentric rings of various electron densities, which is originated from the rough endoplasmic reticulum (rER), and it accumulates prolamins after synthesizing on the ER membrane (Bechtel and Juliano, 1980; Tanaka et al., 1980; Yamagata and Tanaka, 1986; Li et al., 1993; Saito et al., 2012). In contrast to PBI, PBII is a granule with irregular shape, originated from protein storage vacuole (PSV). The diameter of matured PBII typically ranges between 2 to 4 μm, larger than PBI, and glutelin and globulin are both stored in PBII after being synthesized on the rER (Yamagata et al., 1982; Krishnan et al., 1986; Yamagata and Tanaka, 1986; Li et al., 1993). Numerous studies have examined the mutants exhibiting abnormal PB formations (Takemoto et al., 2002; Onda et al., 2009; Wang et al., 2009; Wang et al., 2010; Fukuda et al., 2011; Nagamine et al., 2011; Onda et al., 2011; Ren et al., 2014). Interestingly, these mutations showed chalkiness and are described as "floury endosperm" (Takemoto et al., 2002; Wang et al., 2010; Fukuda et al., 2011; Han et al., 2012; Li et al., 2014; Ren et al., 2014), suggesting that abnormal PB development might be associated with chalky formation in heat-stressed rice. Regarding chalky formation, changes in starch metabolism have received most attention (e.g., Yamakawa et al., 2007; Zhang et al., 2011); however, little has been studied on the possible changes in protein synthesis including PB development. Considering the consistency of the spatial PBs localization of PBs (Ellis et al., 1987;

Hoshikawa, 1989) and chalky zone in the outer endosperms of the dorsal side, we hypothesized that protein synthesis might be cell-specifically suppressed under heat conditions, resulting in an inhibition of PB development prior to chalky formation. Some appropriate cell-specific analysis was required to examine our hypothesis.

Recently, single cell metabolomics has been further expanded due to the technical improvement of the mass analyzers (i.e., Orbitrap mass spectrometer) and applied in plant research (Gholipour et al., 2013; Fujii et al., 2015). A cell pressure probe, originally invented by Steudle's group (Hüsken et al., 1978) and long-used for measuring the cell water status, has been adopted as a picolitre pipette to establish a new type of "analytical method that can be performed in intact plant cells" by combining with an Orbitrap mass spectrometer (Gholipour et al., 2013). More recently, the resolution and sensitivity of the method have been improved by introducing an internal electrode in the capillary holder and adopting the mixture of an ionic solution and the silicone oil in the quartz capillary (Nakashima et al., 2016). This type of cell metabolomics appears to be a robust and powerful method for performing cell-specific analysis. However, most of the cell metabolomics, including this method, have been confined to laboratory use at room temperature. To the best of our knowledge, no attempt has been made to further improve the cell-specific analytical method that allows investigation of metabolic response to some environmental stimuli, such as temperature responses in developing crop plants.

To overcome such limitation at the analysis, we have established a new on-site cell-specific analytical method by combining picolitre pressure-probe-electrospray-ionization mass spectrometry (picoPPESI-MS, referred as 'IEC-PPESI-MS' in Nakashima et al., 2016) with an environment control to be used for conducting a cell-specific analysis in the cells growing under heat conditions, which were expected to form chalkiness. Under the temperature equilibrium conditions, this analytical method allows to perform on-site real-time metabolites profiling in the target endosperm cells growing at a set temperature (i.e., 34°C) without any pretreatments (see Nakashima et al., 2016). By combining with a transmission electron microscopy (TEM), it has been shown for the first time that (i) PSVs could be preserved in the cytosol by osmotic adjustment under heat conditions to lead chalky formation as a heat survival strategy and (ii) N-supplied cells increased protein synthesis rate at high temperature to avoid chalkiness.

Results

Rice Appearance

In both non-heat (26°C) treatment and N application followed by non-heat (N+26°C) treatment, there were essentially no white-back kernels and the same occurrence of perfect kernels was observed (Table 1). Under heat (34°C) treatment, the proportion of white-back kernels (see 34°C in Figure 1B) increased, reaching to 66.4%, and resulted in a substantial decrease in perfect kernels (Table 1). In contrast, N application followed by heat (N+34°C) treatment ameliorated rice appearance by remarkably decreasing white-back kernels, reaching to 7.6%, but with an approximately 40% increase in perfect kernels (Figure 1C). Moreover, partially ameliorated chalky kernels were classified as other kernels. There was no treatment difference between kernel dry weights in both perfect rice and white-back rice (Table 1), although the average dry weight of pooled kernels declined in 34°C and N+34°C treatments (Table 1). No difference was observed on rice appearance between 26°C and N+26°C treatments and therefore, the following experiments were conducted in 26°C, 34°C, and N+34°C treatments.

Microscopic Observations in Chalky Zone

The outer endosperm cells located at the dorsal side, where the high frequency of chalkiness was confirmed at maturation (Table1), were observed microscopically using a light microscope and TEM. Rice grain sections collected in 26°C, 34°C, and N+34°C treatments were dual-stained and observed using a light microscopy, and starch granules and proteins were stained in bluish purple and blue area, respectively (Figures 1D-F). In 26°C treatment, the outer endosperm cells were densely packed mainly with numerous well-developed amyloplasts and mature PBs mostly located at the periphery of cytoplasmic compartments (Figure 1D). Heterogeneity in the size of amyloplasts was contrastingly observed in 34°C treatment as well as a relatively large gap space in the cytoplasmic compartments (see the arrowheads in Figure 1E). Cell morphology in N+34°C treatment was similar to that in 26°C treatment (Figure 1F). The image analysis showed that 34°C treatment significantly reduced areas of amyloplasts and PBs in the cytoplasmic compartments (Figures 1G and H) and resulted in the preservation of over 25% of gap spaces among amyloplasts and PBs inadequately formed in the chalky zone, different from the perfect kernels in 26°C treatment (Figure 1I). In N+34°C treatment, the area-based percentage of amyloplasts and PBs recovered at the similar level to the 26°C treatment (Figure 1G-I). Figure 1I indicates that these modifications of organelle compartmentations observed at high temperature were ameliorated by additional N supply (Figure 1F) and displayed no difference in 26°C treatment (Figure 1I).

In the outer endosperms in 34°C treatment, the gap area was typically located among

145 amyloplasts in the cytosol. Microscopic observation was then made by using TEM in the
146 same zone for each treatment at 12, 20, and 40 DAH (Figures 2A-I). At 12 DAH, the
147 developing PSVs were similarly observed in all treatments. Numerous PSVs, few PBs,
148 mitochondria, and rERs were observed in the cytosol (Figures 2A-C). In contrast to 12 DAH,
149 the ultrastructure of the cells fixed at 20 and 40 DAH both differed between treatments. The
150 majority of PSVs were filled with PBII until 20 DAH in 26°C treatment (Figure 2D), whereas
151 PSVs in 34°C treatment remained in the cytosol, leading to the formation of air spaces at
152 maturation (Figures 2E and H). In N+34°C treatment, normal PBII development was
153 observed with little or no PSVs at 40 DAH, similar to 26°C treatment (Figure 2I). In each
154 treatment, the water content of the kernels decreased through the grain-filling stage, although
155 at maturation, higher water content was observed in 34°C treatment, compared to other two
156 treatments (Figures 2J-L).
157
158 ***In Situ* Turgor Assay in Outer Endosperm Cell Growing under Heat Conditions**
159 In the corresponding target cells at the early stage, where PSVs were similarly localized in
160 all treatments (Figures 2A-C), there were some kernel-to-kernel variations in outer
161 endosperm cell turgor in each treatment (Figure 3B) because each kernel exhibited some
162 variations in the appearance at maturation (Table 1). 34°C-treated cells exhibited positive but
163 relatively low turgor, compared to those in 26°C treatment (Figure 3B). Cell turgor in N+34°C
164 treatment was overall higher in 34°C treatment, maintaining the same level that of 26°C
165 treatment (Figure 3B).
166
167 **On-site Cell-specific Metabolites Profiling in Kernels Growing under Heat Conditions**
168 When the cell sap was directly analyzed using picoPPESI-MS under controlled environments
169 (Supplementary file 1), numerous metabolites (mostly amino acids, sugars, organic acids,
170 and secondary metabolites) were identified in negative ion mode at less than 5 ppm
171 differences from theoretical molecular weight values (Figures 3C-E, Supplementary file 2). In
172 26°C treatment, the peaks of phosphoric, malic, and glutamic acids (as $[M–H]^-$, M=molecular
173 species), and some sugars (as $[M–H]^-$ and/ or $[M+Cl]^-$) were observed in the mass spectrum
174 as major ions (Figure 3C, Supplementary file 2). Under 34°C treatment, the signal intensity
175 of glutamic acid was much higher than in 26°C treatment, and the content of ascorbic acid,
176 glutathione, and amino acids increased as in typical heat responses (Figure 3D,
177 Supplementary file 2). The signal intensities of ascorbic acid and glutathione both involved
178 in the scavenging of reactive oxygen species (ROS) were higher in 34°C treatment than in
179 26°C treatment (Figure 3D; Supplementary file 2). Moreover, the accumulation of cysteine
180 (Cys) that forms the disulfide bridges was observed with over 75% of frequency under 34°C

181 treatment, whereas Cys-related signals were not found in 26°C treatment (Supplementary
182 file 2). In N+34°C treatment, the signal of Cys as $[Cys–H]^-$ was rarely observed (<20%),
183 consistently with those of Cys-sugar cluster ions, such as $[Cys+Hex–H]^-$ and $[Cys+Hex_2–H]^-$,
184 and generated during the ionization process (not detected and 0.09%, respectively; see
185 Supplementary file 2). Higher sugar accumulation than heat was observed under N+34°C
186 treatment (Figure 3E). For methionine (Met) which forms disulfide bonds similarly to Cys, the
187 signal intensities of $[Met–H]^-$ and two Met-sugar cluster ions, $[Met+Hex–H]^-$ and
188 $[Met+Hex_2–H]^-$, were smaller than those of Cys, with no clear differences in the different
189 treatments (Supplementary file 2).
190
191 **Heat and Nitrogen-enhanced Adaptation on Protein Body Development in the**
192 **Endosperm Cells**
193 When exposed to heat, the weight of proteins per kernel decreased. However, the protein
194 weight per kernel in N+34°C treatment was similar to that in 26°C treatment (Figure 4B). The
195 number and area of each PB decreased remarkably in 34°C treatment (Figures 4C-F), and
196 N application increased the number of each PB and area of PBII, but not completely for the
197 area of PBI (Figures 4C-F). The area of PBII in 26°C treatment was approximately 2.5-fold
198 greater than PBI localized in the cells (Figures 4E and F). PBI is composed of two types of
199 layers, namely, the inner Cys-rich 10-kDa prolamins (CysR10P) layer and outer layer
200 containing the mixture of other prolamins (see Figures 2G and I). In 34°C treatment, the
201 apparent area of CysR10P in PBI increased, although the outer layer was decreased
202 remarkably (see deep-colored bars in Figure 4E). In N+34°C treatment, the area of CysR10P
203 in PBI was similar to that in 34°C and prone to be higher than 26°C treatment. Consequently,
204 the area of CysR10P (number x area) in the chalky cells increased due to N application,
205 compared to that in 34°C treatment (Supplementary file 3). There was little effect on the
206 accumulation of glutelin precursors (pro-glutelin) and acidic (α)-glutelin to 34°C, although the
207 content of CysR16P, Cys-poor 13-kDa prolamin (CysP13P), α-globulin, and basic (β)-glutelin
208 decreased in 34°C treatment (Figure 4G). When N was supplied to the soil prior to 34°C
209 treatment, the content of β-glutelin and CysR16P increased to the level of 26°C treatment
210 and greater than that of 34°C treatment (Figure 4G). The accumulation of CysR10P was
211 specifically observed in 34°C treatments (Figure 4G). Analysis of the time course of changes
212 in PSV and PBII (stored in PSV) volumes in the chalky zone showed that the expansion of
213 PSVs in 34°C treatment progressively occurred, reaching 26 fL at maturation, 2.6-fold larger
214 than that in 26°C treatment (Figure 5A). PB accumulation rate retarded in 34°C treatment,
215 compared to that in 26°C treatment (Figure 5B). Additionally, in 26°C and N+34°C treatments
216 there were positive and linear relationships between the entire PSV and PB volumes (inset

in Figure 5C). In contrast, the 34°C-treated PSV volume was shown to be positively correlated with the PSV matrix volume (Figure 5C).

Discussion

Rice chalkiness is a typical physiological disorder of immature kernels and it exhibits air spaces between loosely-packed starch granules causing a random light reflection (Tashiro and Wardlaw, 1991b; Zakaria et al., 2002). Deterioration in the milling quality due to an increase in heat-induced chalky rice has been a serious concern in global rice production under the advancing global warming. N supply decreases heat-induced chalky formation (Perez et al., 1996; Wakamatsu et al., 2008), although the underlying mechanisms of heat-induced chalky formation and the N-enhanced adaptation have never been systematically examined mostly due to the technical difficulties at the cellular level. As pointed previously (Hakata et al., 2017), another difficulty for studying heat-related damages in crop plants would be due to the low reproducibility of high-temperature treatment under field conditions, which implies the need of environmental controls. We have developed a new on-site cell metabolomics performable in the controlled environments to make such a cellular analysis possible (Supplementary file 1). By using this method, we carried out a cell-specific analysis in the putative chalky zone in the attached kernels grown under high-temperature environments, in a combination with a transmission electron microscopy. It has been uncovered that the preservation of relatively large PSVs among loosely-packed starch granules in the cytosol was attributed to the air spaces formed in the dorsal chalky zone in the kernels. Although 34°C-treated cells disturbed protein synthesis, N supply enhanced the protein synthesis rate to sustain normal development of amyloplast and PBs in the zone, leading to the reduction in air spaces under heat conditions. Therefore, we conclude that rice endosperm cells could alter vacuolar morphology by regulating vacuolar trafficking and protein processing as a heat stress adaptation, depending on the available nitrogen level. We also propose that rice chalky formation is a form of heat acclimation.

Establishing an on-site cell-specific analysis to investigate heat-induced damages in rice plants

Recently, single cell metabolomics has been extended mainly due to the introduction of Orbitrap mass analyzer, and this approach has been applied to a number of biological studies including plant cell analysis (Gholipour et al., 2013; Fujii et al., 2015). A cell pressure probe, originally invented by Steudle's group (Hüsken et al., 1978) and long-used to measure the cellular water status in plant sciences, has been adopted as a picolitre pipette to establish a new type of *in-situ* analytical method by combining with an Orbitrap mass spectrometer in

253 Nonami's laboratory (Gholipour et al., 2013). More recently, both resolution and sensitivity of
254 the analytical method have been improved by introducing an internal electrode in the capillary
255 holder and adopting a mixture of an ionic solution and silicone oil in the quartz capillary
256 (Nakashima et al., 2016). This method, called 'picolitre pressure-probe-electrospray-
257 ionization mass spectrometry (picoPPESI-MS)', is performable in intact plants. This type of
258 cell metabolomics appears to be a powerful tool. However, to the best of our knowledge,
259 most existing cell metabolomics, including this method, has been confined to the laboratory
260 use to study cellular metabolisms at room temperature. To date, no attempts have been made
261 on further improvement of the methods to investigate metabolic responses to some
262 environmental stimuli, such as heat responses in developing crop plants that we examined
263 here.
264
265 To meet the requirement, a new on-site cell-specific analytical method has been developed
266 by combining picoPPESI-MS with environment controls (Supplementary file 1). In this system,
267 both developing plants and analytical environment could be equilibrated at the same set
268 temperature. Under temperature equilibrium conditions, a probe tip was finely introduced into
269 the target endosperm cells prior to chalky formation. The picolitre cellular fluids discharged
270 into the quartz capillary were collected, and the metabolome analysis was carried out directly
271 without any pretreatment (see Materials and Methods section). The use of the analytical
272 method at the early ripening stage allowed determination of the differences in metabolites
273 between treatments in the developing dorsal outer endosperm cells, where numerous PBs
274 are known to be localized (Ellis et al., 1987; Hoshikawa, 1989) (Figure 3). As discussed below,
275 it is noteworthy that our cell-specific analysis clarified that the fate of the endosperm cells
276 was determined, in which there were no obvious morphological treatment differences (Figure
277 2A-C).
278
279 **Direct evidence for morphological and metabolic characteristics of chalky formation**
280 **and nitrogen-enhanced adaptive process under heat conditions**
281 Figure 6 shows the likely processes of chalky formation and the N-enhanced adaptation
282 occurring in the outer endosperms cells under heat conditions. Our results provide a new
283 evidence that at high temperature, the volume of PSVs increased through maturation and
284 remained in the cells at maturation, with a limited accumulation of storage proteins, mostly
285 glutelin and globulin (Figures 4 and 5). When N was supplied prior to 34°C treatment, the
286 synthesis of proteins including those storage proteins was sustained under heat conditions,
287 resulting in normal PBII development (Figures 2 and 4E), accompanied with a substantial
288 starch accumulation (Figures 1G and 6) and PBI development (Figures 4C and E,

Supplementary file 3). Under N+34°C treatment, the spatial ratio of the gap spaces at maturation was similar to that of 26°C treatment, 14.8% lower than that of white-back rice harvested in 34°C treatment (Figure 1I). As the results indicated, approximately 70% (Δperfect rice 40.7% · Δwhite-back rice 58.8%$^{-1}$) of white-back rice simply turned into the perfect rice without causing any reduction in kernel weight (Table 1).

It has been shown that heat stress affected the PB development, and the volume of PSVs progressively increased over time, reaching to 2.5-fold larger than PBII in 26°C treatment at maturation (Figures 4F and 5A and B). Based on the observed size and number of each PB (Figures 4C-F), our calculation suggests that the volumetric ratio of PSV to cytosolic volume corresponded to 24.5% on average (ranging between 6.5–46.4%) of cytosol, indicating that PSVs would be a predominant compartment occupying the cytosol at least at maturation. Hence, the observed spatial modifications of vacuolar compartmentation (Figures 1E and 6) account for the gap space formation under heat conditions. Most mutants with abnormal PBII formation showed floury endosperms, whose appearance was opaque (Takemoto et al., 2002; Wang et al., 2010; Fukuda et al., 2011; Ren et al., 2014), whereas a vacuolar processing enzyme, *OsVPE1* knockdown mutant contrastingly produced translucent kernels (Wang et al., 2009). Given the fact that OsVPE1 plays a role in the maturation of glutelin transported into PSV as Cys protease in the final stage of PB development (Wang et al., 2009), it is not surprising that unlike other enzymes, VPE does not have a dramatic volumetric impact on chalky formation. Thus, the results of Wang et al. (2009) do not necessarily conflict with our conclusion.

Osmotic adjustment occurs in the growing cells at moderately low water potential (Morgan, 1977; Cutler et al., 1980a, 1980b; Meyer and Boyer, 1981). During the osmotic adjustment, turgor pressure can be maintained by accumulating osmotically active solutes, such as sugars and amino acids, into the cells (Morgan, 1977; Meyer and Boyer, 1981). As reported previously (Wada et al., 2011; Wada et al., 2014), osmotic adjustment also occurred in the rice endosperms cells growing under dry wind conditions prior to chalky ring formation. On-site cell metabolomics and *in situ* turgor assay conducted in outer endosperms indicated clear treatment differences in the heat adaptive responses (Figure 3B-E). Different from the drought-related studies, there seem to be few studies regarding osmotic adjustment under heat conditions (e.g., Jiang and Huang, 2000 in turfgrass). In this study, the determination of cell osmotic pressure was not attainable using a freezing point osmometer, because of the interference of starches contained in the sap. However, based on the treatment differences in metabolites in the target zone, it was reasonably interpreted that N-treated cells strongly

325 adjusted osmotically to maintain the protein synthesis rate at high temperature, whereas
326 under low N level, the cells adjusted less osmotically and the protein synthesis rate slowed
327 down, and therefore the energy requirement in cytosol could be maintained low.
328
329 Cys stabilizes the tertiary structure of proteins through the formation of disulfide bonds, which
330 is necessary for protein folding and the modulation of enzyme activity in the cells. N-induced
331 increase in Cys-rich 10-kDa prolamin in PBI (Figure 4E) and the result of SDS-PAGE (Figure
332 4G) are strong evidence supporting our conclusion. The results of cellular metabolome
333 analysis suggest that during the N-enhanced adaptation process, Cys would have
334 contributed to vacuolar trafficking and protein processing without participating in osmotic
335 adjustment as an osmotically active solute. The greater abundance of Cys-related signals
336 was frequently observed in the heat-treated cells, but no or less in other two treatments (see
337 $[Cys–H]^-$, $[Cys+Hex–H]^-$, and $[Cys+Hex_2–H]^-$ in Supplementary file 2). And, this data
338 corresponds to the occurrence of white-back kernels (Table 1). Hence, it is expected that
339 higher Cys accumulation would have occurred in the cytosol in 34°C treatment, as well as
340 sugars and other major amino acids, which might be caused by a low assimilate input under
341 long-term heat conditions. It appeared that N application increased amyloplast development
342 in the cells under heat conditions (Figure 1G), and hence the effects of N supply were large
343 enough to structurally stabilize the activity of a series of starch biosynthesis-related enzymes
344 under heat conditions, together with PB development.
345
346 For nitrogen budget in the cells, it remains questionable how much N had been synthesized
347 into the storage proteins during the adaptation process. In the comparative analysis between
348 34°C and N+34°C treatments, our TEM image analysis indicated that the treatment difference
349 in the spatial ratio of PBI and PBII occupied in the cells was 0.52% and 3.86% on average,
350 respectively. The percentage of the chalky area to the transversal area corresponds to 17.4
351 ± 0.8% (mean ± SD, n = 18). The mean area of the transversal section measured in 34°C-
352 and N+34°C-treated kernels was 0.051 and 0.050 cm^2, respectively, and the averaged
353 longitudinal kernel length in these treatments was 5.15 and 5.16 mm, respectively. With the
354 specific gravity of PBI and PBII, 1.27 and 1.29 $g{\cdot}mL^{-1}$, respectively (Tanaka et al., 1980), the
355 weight difference in the chalky zone between those treatments corresponded to 0.32
356 $mg{\cdot}chalky\ zone^{-1}$. Because the treatment difference in the protein content was 0.25
357 $mg{\cdot}kernel^{-1}$ (Figure 4B) and the difference in the occurrence of white-back rice was 58.8%
358 (Table 1), our estimation suggests that in N+34°C treatment approximately 75.1% of proteins
359 increased by N application were synthesized as storage proteins in the PBs to fill up the gap
360 spaces in the chalky zone. However, the rest of 24.9% was consumed for synthetizing PBs

361 in other area and other enzymes, mostly for starch synthesis.
362
363 **The adaptation strategies of rice endosperms to heat conditions**
364 There is a large body of evidence that ROS, such as hydrogen peroxide, play a role as
365 important second messengers in signal transduction networks associated with
366 developmental processes or in response to abiotic stress (Mittler et al., 2004; Skopelitis et
367 al., 2006). Generated hydrogen peroxide might serve as a signal introducing the programmed
368 cell death and subsequently kernel desiccation (Onda et al., 2009). More recently, Ibl et al.
369 (2014) suggested that both the membrane shrinkage and degeneration of PB occurred
370 before PB development were completed in barley endosperm cells. The synthesis of vast
371 amounts of disulfide-rich storage proteins during grain-filling (Figure 4E and G) might be
372 accompanied by the production of hydrogen peroxide in ER, resulting in the peroxidation of
373 membrane lipids under normal conditions (Sattler et al., 2006; Onda et al., 2009). In contrast,
374 the behavior of PSVs we observed (Figures 2H and 5) suggests that heat might have
375 disturbed the cellular redox status to inhibit the peroxidation of membrane lipids under heat
376 conditions. PSVs treated at 34°C were found to be expanding over time, but with a retardation
377 of PB accumulation (Figure 5A and B). Importantly, the volumetric increase in PSV could be
378 explained by increasing PSV matrix (see Figure 5C), indicating that substantial amount of
379 water had been entering PSVs towards maturation to increase the vacuolar volume. Thus, it
380 is quite unlikely that tonoplast membrane lipids were degraded under heat conditions. One
381 plausible explanation is that a partial degradation of PBII in PSV would occur through the
382 activation of proteases or the autophagy-like process, leading to an increase in the vacuolar
383 osmotic pressure. This would promote water entry into PSVs to sustain the vacuolar volume,
384 and maintain the cell volume. The source of water accumulated in the PSV matrix remains
385 unknown. However, based on the increases in the content of ascorbate, glutathione, and
386 monodehydroascorbate detected at the cellular level (Supplementary file 2), we speculate
387 that the accumulation might be a consequence of an increased activity of ascorbate
388 peroxidase catalyzing the conversion of hydrogen peroxide into water. PB development
389 sustained during the N-enhanced adaptation process supports our conclusion that disulfide
390 bond formation and tonoplast denaturation would be facilitated by strong osmotic adjustment
391 (Figure 2). As observed in Figure 2J-L, 34°C-treated kernels exhibited higher water content
392 than 26°C treatment, consistent with previous studies (Ishimaru et al., 2009; Iwasawa et al.,
393 2013; Hayashi et al., 2015). Given the fact that water is a major compound in both PSV matrix
394 and vacuoles in the gap spaces, it is not surprising that chalky zone (or even chalky rice)
395 exhibited relatively high moisture content under heat conditions, compared to 26°C treatment.
396 Storing water in the endosperms along the dorsal vasculature may be an essential event to

397 sustain embryo development in the seeds exposed to the extremely high temperature, as
398 heat-induced precocious germinations were similarly observed in rice (Iwasawa et al., 2013)
399 and oilseed rape seeds (Brunel-Muguet et al., 2015). Hence, we propose that chalkiness is
400 a form of acclimation to heat stress.
401
402 **Threshold of chalkiness and other possible candidate organelle involved in chalkiness**
403 Regarding the threshold above which chalkiness appears, our image analysis suggests that
404 the transition between chalk and translucence corresponds to a range between 10.3 and
405 25.1% in N+34°C treatment and 34°C treatment, respectively (see Figure 1I). In another type
406 of chalkiness, called milky-white rice, chalkiness was observed at 13.3% on average (Wada
407 et al., 2014). Taken together, significant transparency loss would occur in a range of 10.3 to
408 13.3%. The preservation of PSVs expanded in cytosol was responsible for the formation of
409 heat-induced white-back rice (Figure 6). In the chalky zone, a small number of cells,
410 corresponding to 3.4% of the total chalky area (see the red area in Supplementary file 4A)
411 and located adjacent to the sub-aleurone layer, retained some large lytic vacuoles in addition
412 to PSVs (Supplementary file 4H). This observation has risen a possibility that in 'Koshihikari',
413 some vacuoles might also have participated in the air space formation. Similarly, we
414 previously showed that the presence of vacuoles stayed in the cytosol at osmotic adjustment
415 might have an impact on the formation of air spaces in the inner endosperm cells in a foehn-
416 induced chalky ring formation (Wada et al., 2014). Wakamatsu et al. (2008) reported a clear
417 varietal difference in the occurrence of white-back rice when the same amount of N was
418 applied under heat conditions; however, the underlying mechanisms remain unclear. Some
419 morphological differences may explain the difference that is currently under investigation.
420 More recently, it has been possible to trace metabolites in the target zone using the stable
421 isotope(s) in mass spectrometry (Wada et al., 2017). The use of this analytical method may
422 extend our understanding of heat adaptation mechanisms in rice endosperms.
423
424 **Conclusion and remarks**
425 In this work, the on-site cell-specific analysis was utilized to investigate the cellular
426 mechanisms of heat-induced chalky formation and N-enhanced adaptation response.
427 Combined analysis with a TEM demonstrated that the cells adjusted less osmotically and
428 reduced protein synthesis to retain PSVs in the cells at low N level under heat conditions,
429 and that N supply enhanced the heat tolerance and the cells sustained protein synthesis
430 during strong osmotic adjustment at high temperature. During the N-enhanced adaptation
431 process, the formation of disulfide bonds was promoted by consuming Cys to sustain normal
432 PB and amyloplast development even under heat conditions, which resulted in a remarkable

increase in perfect rice. Hence, the extent of translucent loss in endosperms could result from the spatial modifications of organelle compartments, closely associated with available N level in the cells. Our on-site cell-specific analysis can be applied in a number of cell-specific studies in future, including heat-induced rice spikelet sterility. Finally, to our knowledge, no attempts have been made in other instruments such as a nuclear magnetic resonance. However, a similar combination with environmental controls may be useful in the field of environmental plant biology, particularly when investigating temperature stress responses in crop plants, as reported here.

Materials and Methods

Plant materials

Oryza sativa L. 'Koshihikari' potted plants were grown without giving a top dressing in Kyushu Okinawa Agricultural Research Center, Chikugo, Japan, according to the method of Wada et al. (2011). At flowering, the potted plants grown in field were transferred to the walk-in environmentally-controlled growth chamber (26/22°C, 70/80% relative humidity, and 750 μmol photons m^{-2} s^{-1} photosynthetically active radiation [PAR]) set at the plant canopy using light emitting plasma (LEP) lamps (STA 41-02, Stray Light Optical Technologies, Inc., IN, the US) with a photoperiod of 13 h day/11 h night. For half of the potted plants, 0.45 g·pot^{-1} of urea was applied at 4 DAH to examine the effects of N application under heat conditions on rice quality. At 5 DAH, half of the plants were transferred to another growth chamber set at 34°C and 70% relative humidity (RH) (09:00−15:00) / 28°C and 80% RH (15:00−09:00) and 750 μmol m^{-2} s^{-1} PAR with the same photoperiod to be treated at high temperature for 10 days (referred to as '34°C treatment'). Other potted plants were kept in the same chamber in a non-heat (26°C) treatment. At 15 DAH, plants were transferred to the control chamber to grow until the mature stage (typically 40 DAH).

On-site cell metabolomics and turgor assay

On-site live cell metabolome analysis using picolitre pressure-probe-electrospray-ionization mass spectrometry (picoPPESI-MS, Nakashima et al., 2016) was carried out in the dorsal outer endosperm cells of the superior kernels attached to the upper position of a panicle, where a high frequency of chalkiness was observed under 34°C treatment (Table 1). Simply, the system was composed of picoPPESI-MS and two measurement rooms individually attached to growth chambers (K260B029-S01, Tsubuku Corporation Ltd., Kurume, Japan) (see Supplementary file 1). The combination of the environmental control and picoPPESI-MS allowed us to directly perform cell metabolites profiling real-time at the target zone without

468 any pretreatments under each set environmental conditions. Potted plants at 11−12 DAH
469 were moved to the measurement room where they were placed at the center of a U-shaped
470 vibration-free table (HOA-0808LA(Y), Herts Co. Ltd., Yokohama, Japan) in the measurement
471 room. Temperature change in the growth chamber disturbs cell pressure probe measurement
472 (Boyer, 1995), and therefore the following assays were initiated, at which the pressure probe
473 system and plants reached to the temperature equilibrium (typically in 30 min). Prior to the
474 assay, a part of the hull (i.e., palea) in the attached kernels was quickly and gently removed
475 under humid conditions (Wada et al., 2011). In the preliminary experiment, it was observed
476 that there were distinct tissue-to-tissue variations in metabolites between the pericarp
477 (Supplementary file 5) and outer endosperm cells (Figures 3C-E). When the kernel score
478 reached to 0.9 (see Figure 1 in Wada et al., 2014), a 1 mm diameter biopsy punch was used
479 to remove 0.031 cm^2 of pericarp tissue in the dorsal side of the kernel to obtain the sap from
480 the endosperm cells under humid conditions prior to the capillary tip insertion (Figure 3A).
481 Therefore, a possible contamination could be ruled out from the pericarp cell layers. The
482 kernel was gently fixed on the sample holder using tape and magnets (Supplementary file 1).
483 The tip of microcapillary filled with 0.01% (v/v) ionic liquid/silicone oil mixture was impaled
484 into endosperm cells (typically between 50-150 μm below nucellar-epidermis) with the aid of
485 a motorized piezomanipulator (DC-3K, Märzhäuser Wetzlar, Germany). Cell sap was
486 collected by depressurizing in the microcapillary, and the tip immediately oriented toward the
487 orifice of an Orbitrap mass spectrometer (Q-Exactive, Thermo Fisher Scientific Inc., MA, the
488 US) was electrified with −4 kV using a high voltage generator (AKTB-05k1PN/S, Touwa
489 Keisoku Corp., Tokyo, Japan). The MS scan was performed in negative ion mode with the
490 instrumental settings of 200 ms as maximum injection time, inlet ion transfer tube
491 temperature of 250°C, and resolution of 35,000. When the target cells were successfully
492 impaled to collect picolitre cell sap without tip plugging, the entire process of picoPPESI-MS
493 analysis on the cells was completed within few minutes. All the standard chemicals and
494 organic solvents used in the experiments were liquid chromatography-mass spectrometry
495 (LC/MS) grade and purchased from Wako Pure Chemical Industries, Ltd. (Osaka, Japan).
496 Ultrapure water of 18.2 MΩ cm^{-1} was used throughout the experiment. For picoPPESI-MS
497 operation, an ionic liquid, trihexyl (tetradecyl) phosphonium bis trifluoromethanesulfonyl
498 amide (Cyphos IL109 Strem Chemicals Inc., MA, the US) was suspended in phenyl methyl
499 silicone oil (Wacker silicone fluid AS4, Munich, Germany) at a concentration of 0.01% (v/v)
500 to enhance electric conductivity of the silicone oil. All manipulations were conducted under a
501 digital microscope (KH-8700, HiRox Co. Ltd., Tokyo, Japan), and kernels attached to the
502 sample holder was humidified during all processes. In addition to the picoPPESI-MS analysis,
503 *in situ* cell turgor in both pericarp and outer endosperm located at the same dorsal side of

504 the kernels was independently assayed under humid conditions without removing the
505 pericarp, as described previously (Wada et al., 2011, 2014).
506
507 **Microscopy**
508 Kernel samples for microscopic observation were sampled in growth chambers, fixed and
509 embedded according to the method of Saito et al. (2014) with slight modifications. Transverse
510 segments (1−2 mm thick) from the middle of the kernel at 12, 20, and 40 DAH were fixed
511 with 4% (w/v) paraformaldehyde in 100 mM sodium phosphate (pH 7.2) for 3 h at room
512 temperature and then washed in 100 mM phosphate buffer (pH 7.2). Fixed tissues were
513 dehydrated through an ethanol series, and embedded in LR White resin (London Resin,
514 Hampshire, the UK) by two-days polymerizing at 60°C. Semi-thin sections (appropriately 900
515 nm) for light microscopy were stained with 0.1% (w/v) Coomassie Brilliant Blue for 1h
516 followed by potassium iodide for 1min, and ultra-thin sections (appropriately 80−100 nm) for
517 electron microscopy were stained with lead citrate. After the staining, ultra-thin sections were
518 observed with a transmission electron microscope (TEM; JEM-1010, JEOL Ltd., Tokyo,
519 Japan). For the organelle arrangement image analysis, the outline of all amyloplasts, protein
520 bodies, and other area (referred to as 'gap') on the light microscopic images, and the area of
521 both PBs on TEM images were traced by using ImageJ software (US National Institutes of
522 Health, Bethesda, MD, the US). The outline of PSV and PBII in PSV was also traced. By
523 assuming that they were spherical with a same r, the ratio of volume ($V=4/3\pi r^3$) to the area
524 ($A=\pi r^2$) was $4/3r$. This value was regarded as the representative ratio to calculate V from A
525 with the conversion, $V= 4/3rA$. The volume of PSV matrix was calculated as the difference
526 between PSV and PBII volumes.
527
528 **Protein Extraction from Rice Kernels and SDS-PAGE**
529 In each treatment, one-third of the kernel containing the dorsal side of the matured kernels,
530 corresponding to the chalky zone of white-back rice, was removed using a razor blade. Total
531 proteins were extracted from the kernel section in 50 mM Tris-HCl, pH 6.8, 100 mM DTT, 8
532 M urea, 4% (w/v) SDS, and 10% (v/v) glycerol. Proteins were separated by SDS-PAGE with
533 10−20% acrylamide and stained with Coomassie Brilliant Blue.
534
535 **Kernel Quality and Weight**
536 Spikelets in each portion of a panicle were further classified according to the method of
537 Matsuba (1991). The appearance of dehulled grains (the numbers of white-back kernels)
538 was visually evaluated with >1.8mm thickness of grains, according to the standard evaluation
539 method of The Ministry of Agriculture, Forestry and Fisheries of Japan

(http://www.maff.go.jp/j/seisan/syoryu/kensa/pdf/genmai_kaisetsu.pdf). The dry weight of kernel samples was determined during the treatment and at harvest, as described previously (Wada et al., 2011).

Nitrogen and Starch Content Assay

The protein content of kernels is conventionally estimated using an N-protein conversion factor, 5.95 from the N content determined by the Kjeldahl method.

Statistical Analysis

Statistical analysis of all other data was conducted using a Tukey's test in a general linear model (GLM) procedure in JMP software (version 12.1.0, SAS Institute Inc., Cary, NC).

Acknowledgements

The authors thank Ms. Fujiko Komiya, Mr. Makoto Nakajima, and Mr. Keiji Miike for their help in growing the rice plants and assistance with the experiments. This work was supported by JSPS KAKENHI Grant Number 16H02533 and 17H03759. RE-B is a research member of National Council of Scientific and Technological Research (CONICET), Argentina.

References

Bechtel DB, Juliano BO (1980) Formation of protein bodies in the starchy endosperm of rice (*Oryza sativa* L.): A re-investigation. Annals of Botany **45:** 503-509

Boyer JS (1995) Measuring the water status of plants and soils. Academic Press, San Diego, California.

Brunel-Muguet S, D'Hooghe P, Bataille MP, Larre C, Kim TH, Trouverie J, Avice JC, Etienne P, Durr C (2015) Heat stress during seed filling interferes with sulfur restriction on grain composition and seed germination in oilseed rape (*Brassica napus* L.). Frontiers in Plant Science **6:** 213

Cutler JM, Shahan KW, Steponkus PL (1980a) Alteration of the internal water relations of rice in response to drought hardening. Crop Science **20:** 307-310

Cutler JM, Shahan KW, Steponkus PL (1980b) Dynamics of osmotic adjustment in rice. Crop Science **20:** 310-314

Ellis JR, Gates PJ, Boulter D (1987) Storage-protein deposition in the developing rice caryopsis in relation to the transport tissues. Annals of Botany **60:** 663-670

Fujii T, Matsuda S, Tejedor ML, Esaki T, Sakane I, Mizuno H, Tsuyama N, Masujima T (2015) Direct metabolomics for plant cells by live single-cell mass spectrometry. Nature Protocols **10:** 1445-1456

Fukuda M, Satoh-Cruz M, Wen LY, Crofts AJ, Sugino A, Washida H, Okita TW, Ogawa M, Kawagoe Y, Maeshima M, Kumamaru T (2011) The small GTPase Rab5a is essential for intracellular transport of proglutelin from the Golgi apparatus to the protein storage vacuole and endosomal membrane organization in developing rice endosperm. Plant Physiology **157:** 632-644

Gholipour Y, Erra-Balsells R, Hiraoka K, Nonami H (2013) Living cell manipulation, manageable sampling, and shotgun picoliter electrospray mass spectrometry for profiling metabolites. Analytical Biochemistry **433:** 70-78

Hüsken D, Steudle E, Zimmermann U (1978) Pressure probe technique for measuring water relations of cells in higher-plants. Plant Physiology **61:** 158-163

Hakata M, Wada H, Masumoto-Kubo C, Tanaka R, Sato H, Morita S (2017) Development of a new heat tolerance assay system for rice spikelet sterility. Plant Methods **13**

589 **Han XH, Wang YH, Liu X, Jiang L, Ren YL, Liu F, Peng C, Li JJ, Jin XM, Wu FQ, Wang**
590 **JL, Guo XP, Zhang X, Cheng ZJ, Wan JM** (2012) The failure to express a protein
591 disulphide isomerase-like protein results in a floury endosperm and an endoplasmic
592 reticulum stress response in rice. Journal of Experimental Botany **63:** 121-130
593 **Hayashi H, Ishikawa-Sakurai J, Murai-Hatano M, Ahamed A, Uemura M** (2015)
594 Aquaporins in developing rice grains. Bioscience Biotechnology and Biochemistry
595 **79:** 1422-1429
596 **Herman EM, Larkins BA** (1999) Protein storage bodies and vacuoles. Plant Cell **11:** 601-
597 613
598 **Hoshikawa K** (1989) The growing rice plant : an anatomical monograph. Nobunkyo, Tokyo
599 **Ibl V, Kapusi E, Arcalis E, Kawagoe Y, Stoger E** (2014) Fusion, rupture, and degeneration:
600 the fate of *in vivo*-labelled PSVs in developing barley endosperm. Journal of
601 Experimental Botany **65:** 3249-3261
602 **Ishimaru T, Horigane AK, Ida M, Iwasawa N, San-oh YA, Nakazono M, Nishizawa NK,**
603 **Masumura T, Kondo M, Yoshida M** (2009) Formation of grain chalkiness and
604 changes in water distribution in developing rice caryopses grown under high-
605 temperature stress. Journal of Cereal Science **50:** 166-174
606 **Iwasawa N, K. Horigane A, Ono H, Sekiyama Y, Umemoto T, Yoshida M, Kondo M** (2013)
607 Increase of moisture content and occurrence of precocious germination in rice
608 ovaries during the ripening period under high temperature. Abstracts of Meeting of
609 the Crop Science Society of Japan **235:** 412
610 **Jiang YW, Huang BR** (2000) Effects of drought or heat stress alone and in combination on
611 kentucky bluegrass. Crop Science **40:** 1358-1362
612 **Juliano BO** (1985) Rice : chemistry and technology, Ed 2nd Edn. American Association of
613 Cereal Chemists, St. Paul, Minnesota
614 **Krishnan HB, Franceschi VR, Okita TW** (1986) Immunochemical studies on the role of the
615 Golgi complex in protein-body formation in rice seeds. Planta **169:** 471-480
616 **Li XX, Franceschi VR, Okita TW** (1993) Segregation of storage protein mRNAs on the rough
617 endoplasmic reticulum membranes of rice endosperm cells. Cell **72:** 869-879
618 **Li YB, Fan CC, Xing YZ, Yun P, Luo LJ, Yan B, Peng B, Xie WB, Wang GW, Li XH, Xiao**
619 **JH, Xu CG, He YQ** (2014) Chalk5 encodes a vacuolar H^+-translocating
620 pyrophosphatase influencing grain chalkiness in rice. Nature Genetics **46:** 657-657
621 **Matsuba K** (1991) The morphogenetic mechanism of formation of the panicle branching
622 system in rice plants (*Oryza sativa* L.) (In Japanese with English abstract). Bulletin
623 of the Chugoku Agricultural Experiment Station**:** 11-58
624 **Meyer RF, Boyer JS** (1981) Osmoregulation, solute distribution, and growth in soybean

625 seedlings having low water potentials. Planta **151:** 482-489
626 **Mittler R, Vanderauwera S, Gollery M, Van Breusegem F** (2004) Reactive oxygen gene
627 network of plants. Trends in Plant Science **9:** 490-498
628 **Morgan JM** (1977) Differences in osmoregulation between wheat genotypes. Nature **270:**
629 234-235
630 **Morita S, Wada H, Matsue Y** (2016) Countermeasures for heat damage in rice grain quality
631 under climate change. Plant Production Science **19:** 1-11
632 **Nagamine A, Matsusaka H, Ushijima T, Kawagoe Y, Ogawa M, Okita TW, Kumamaru T**
633 (2011) A role for the cysteine-rich 10 kDa prolamin in protein body I formation in rice.
634 Plant and Cell Physiology **52:** 1003-1016
635 **Nakashima T, Wada H, Morita S, Erra-Balsells R, Hiraoka K, Nonami H** (2016) Single-cell
636 metabolite profiling of stalk and glandular cells of intact trichomes with internal
637 electrode capillary pressure probe electrospray ionization mass spectrometry.
638 Analytical Chemistry **88:** 3049-3057
639 **Onda Y** (2013) Oxidative protein-folding systems in plant cells. Int J Cell Biol **2013:** 585431
640 **Onda Y, Kumamaru T, Kawagoe Y** (2009) ER membrane-localized oxidoreductase Ero1 is
641 required for disulfide bond formation in the rice endosperm. Proceedings of the
642 National Academy of Sciences of the United States of America **106:** 14156-14161
643 **Onda Y, Nagamine A, Sakurai M, Kumamaru T, Ogawa M, Kawagoe Y** (2011) Distinct
644 roles of protein disulfide isomerase and P5 sulfhydryl oxidoreductases in multiple
645 pathways for oxidation of structurally diverse storage proteins in rice. Plant Cell **23:**
646 210-223
647 **Perez CM, Juliano BO, Liboon SP, Alcantara JM, Cassman KG** (1996) Effects of late
648 nitrogen fertilizer application on head rice yield, protein content, and grain quality of
649 rice. Cereal Chemistry **73:** 556-560
650 **Ren YL, Wang YH, Liu F, Zhou KN, Ding Y, Zhou F, Wang Y, Liu K, Gan L, Ma WW, Han**
651 **XH, Zhang X, Guo XP, Wu FQ, Cheng ZJ, Wang JL, Lei CL, Lin QB, Jiang L, Wu**
652 **CY, Bao YQ, Wang HY, Wan JM** (2014) *GLUTELIN PRECURSOR*
653 *ACCUMULATION3* encodes a regulator of post-Golgi vesicular traffic essential for
654 vacuolar protein sorting in rice endosperm. Plant Cell **26:** 410-425
655 **Saito Y, Shigemitsu T, Yamasaki R, Sasou A, Goto F, Kishida K, Kuroda M, Tanaka K,**
656 **Morita S, Satoh S, Masumura T** (2012) Formation mechanism of the internal
657 structure of type I protein bodies in rice endosperm: relationship between the
658 localization of prolamin species and the expression of individual genes. Plant Journal
659 **70:** 1043-1055
660 **Sattler SE, Mene-Saffrane L, Farmer EE, Krischke M, Mueller MJ, DellaPenna D** (2006)

661 Nonenzymatic lipid peroxidation reprograms gene expression and activates defense
662 markers in Arabidopsis tocopherol-deficient mutants. Plant Cell **18:** 3706-3720
663 **Shewry PR, Halford NG** (2002) Cereal seed storage proteins: structures, properties and
664 role in grain utilization. Journal of Experimental Botany **53:** 947-958
665 **Skopelitis DS, Paranychianakis NV, Paschalidis KA, Pliakonis ED, Delis ID,**
666 **Yakoumakis DI, Kouvarakis A, Papadakis AK, Stephanou EG, Roubelakis-**
667 **Angelakis KA** (2006) Abiotic stress generates ROS that signal expression of anionic
668 glutamate dehydrogenases to form glutamate for proline synthesis in tobacco and
669 grapevine. Plant Cell **18:** 2767-2781
670 **Takemoto Y, Coughlan SJ, Okita TW, Satoh H, Ogawa M, Kumamaru T** (2002) The rice
671 mutant *esp2* greatly accumulates the glutelin precursor and deletes the protein
672 disulfide isomerase. Plant Physiology **128:** 1212-1222
673 **Tanaka K, Sugimoto T, Ogawa M, Kasai Z** (1980) Isolation and characterization of two
674 types of protein bodies in the rice endosperm. Agricultural and Biological Chemistry
675 **44:** 1633-1639
676 **Tashiro T, Wardlaw IF** (1991a) The effect of high temperature on the accumulation of dry
677 matter, carbon and nitrogen in the kernel of rice. Functional Plant Biology **18:** 259-
678 265
679 **Tashiro T, Wardlaw IF** (1991b) The effect of high-temperature on kernel dimensions and the
680 type and occurrence of kernel damage in rice. Australian Journal of Agricultural
681 Research **42:** 485-496
682 **Wada H, Masumoto-Kubo C, Gholipour Y, Nonami H, Tanaka F, Erra-Balsells R,**
683 **Tsutsumi K, Hiraoka K, Morita S** (2014) Rice chalky ring formation caused by
684 temporal reduction in starch biosynthesis during osmotic adjustment under foehn-
685 induced dry wind. PLoS ONE **9:** e110374
686 **Wada H, Masumoto-Kubo C, Tsutsumi K, Nonami H, Tanaka F, Okada H, Erra-Balsells**
687 **R, Hiraoka K, Nakashima T, Hakata M, Morita S** (2017) Turgor-responsive starch
688 phosphorylation in *Oryza sativa* stems: A primary event of starch degradation
689 associated with grain-filling ability. PloS ONE **12:** e0181272
690 **Wada H, Nonami H, Yabuoshi Y, Maruyama A, Tanaka A, Wakamatsu K, Sumi T,**
691 **Wakiyama Y, Ohuchida M, Morita S** (2011) Increased ring-shaped chalkiness and
692 osmotic adjustment when growing rice grains under foehn-induced dry wind condition.
693 Crop Science **51:** 1703-1715
694 **Wakamatsu K, Sasaki O, Uezono I, Tanaka A** (2008) Effect of the amount of nitrogen
695 application on occurrence of white-back kernels during ripening of rice under high-
696 temperature conditions. Japanese Journal of Crop Science **77:** 424-433

Wang YH, Ren YL, Liu X, Jiang L, Chen LM, Han XH, Jin MN, Liu SJ, Liu F, Lv J, Zhou KN, Su N, Bao YQ, Wan JM (2010) OsRab5a regulates endomembrane organization and storage protein trafficking in rice endosperm cells. Plant Journal **64:** 812-824

Wang YH, Zhu SS, Liu SJ, Jiang L, Chen LM, Ren YL, Han XH, Liu F, Ji SL, Liu X, Wan JM (2009) The vacuolar processing enzyme OsVPE1 is required for efficient glutelin processing in rice. Plant Journal **58:** 606-617

Yamagata H, Sugimoto T, Tanaka K, Kasai Z (1982) Biosynthesis of storage proteins in developing rice seeds. Plant Physiology **70:** 1094-1100

Yamagata H, Tanaka K (1986) The site of synthesis and accumulation of rice storage proteins. Plant and Cell Physiology **27:** 135-145

Yamakawa H, Hirose T, Kuroda M, Yamaguchi T (2007) Comprehensive expression profiling of rice grain filling-related genes under high temperature using DNA microarray. Plant Physiology **144:** 258-277

Zakaria S, Matsuda T, Tajima S, Nita Y (2002) Effect of high temperature at ripening stage on the reserve accumulation in seed in some rice cultivars. Plant Production Science **5:** 160-168

Zhang GY, Cheng ZJ, Zhang X, Guo XP, Su N, Jiang L, Mao L, Wan JM (2011) Double repression of soluble starch synthase genes SSIIa and SSIIIa in rice (*Oryza sativa* L.) uncovers interactive effects on the physicochemical properties of starch. Genome **54:** 448-459

Author contributions

Hiroshi Wada, Conceptualization, Investigation, Formal analysis, Methodology, Project administration, Supervision, Writing – original draft, Writing – review and editing; Yuto Hatakeyama, Investigation, Formal analysis, Methodology, Writing – original draft, Writing – review and editing; Yayoi Onda, Investigation, Funding acquisition; Writing – review and editing; Hiroshi Nonami, Funding acquisition; Writing – review and editing; Taiken Nakashima, Investigation, Funding acquisition, Writing – review and editing; Rosa Erra-Balsells, Methodology, Writing – review and editing; Satoshi Morita, Methodology, Validation, Writing – review and editing; Kenzo Hiraoka, Methodology, Funding acquisition, Writing – review and editing; Fukuyo Tanaka, Investigation, Writing – review and editing; Hiroshi Nakano, Validation, Writing – review and editing

733 **Additional files**

734

735 **Supplementary files**

736 Supplementary file 1. Diagram of the side view of the on-site cell metabolomics system
737 placed in the laboratory (A) and expanded figure of picoPPESI-MS shown in red rectangle in
738 A (B).

739

740 Supplementary file 2. List of amino acids and carbohydrates detected, as independent ions
741 of clusters, in outer endosperm in each treatment using picoPPESI-MS in negative ion mode.

742

743 Supplementary file 3. Calculated area of PBI (A) and PBII (B) per outer endosperm cell at
744 40 DAH shown in Fig. 2G, H, I. Each parameter was calculated by multiplying the number
745 and the averaged area of each PB.

746

747 Supplementary file 4. The transverse sections of heat-treated kernels collected at 20 DAH
748 (A). In A, black square corresponds to the area used for light microscopic observation (C-K).
749 Area-based percentage of each organelle per cell in a part of chalky zone (traced in red in A)
750 at 20 DAH was shown in B.

751

752 Supplementary file 5. PicoPPESI-MS negative ion mode mass spectra obtained from the
753 pericarp cells in 26°C (C), 34°C (D), and N+34°C (E) at the same stage. Data are
754 representative of similar experiments with 4-5 kernels in each treatment.

755

756

757

758

759

Table 1. Filled kernels, rice appearance including the occurrence of perfect kernel and white-back kernel, and kernel weight in 26°C, N+26°C, 34°C, and N+34°C treatments.

Treatment	Filled kernels	Appearance of brown rice			Kernel dry weight			
		Perfect kernels	White-back kernels	Other kernels	Perfect kernels	White-back kernels	Other kernels	Average
	%				$mg \cdot kernel^{-1}$			
26°C	97.9	100.0a	0.0b	0.0a	21.6	-	-	21.7a
N+26°C	96.5	98.9a	0.0b	1.1a	21.8	-	22.7a	21.8a
34°C	94.4	11.4c	66.4a	22.2a	19.9	20.2	20.2b	20.2b
N+34°C	94.7	52.1b	7.6b	40.4b	20.2	20.7	20.0b	20.2b

Values in appearance are means measured from superior kernels attached to the upper position of a panicle from 3-5 panicles in each treatment. The dry weight of each kernel type was means of individually collected 3-7 panicles, and the average dry weight was calculated in each treatment. Means within a column followed by different letters indicate a significant difference (p <0.05) (Tukey's Honestly Significant Difference [HSD]).

Figure 1

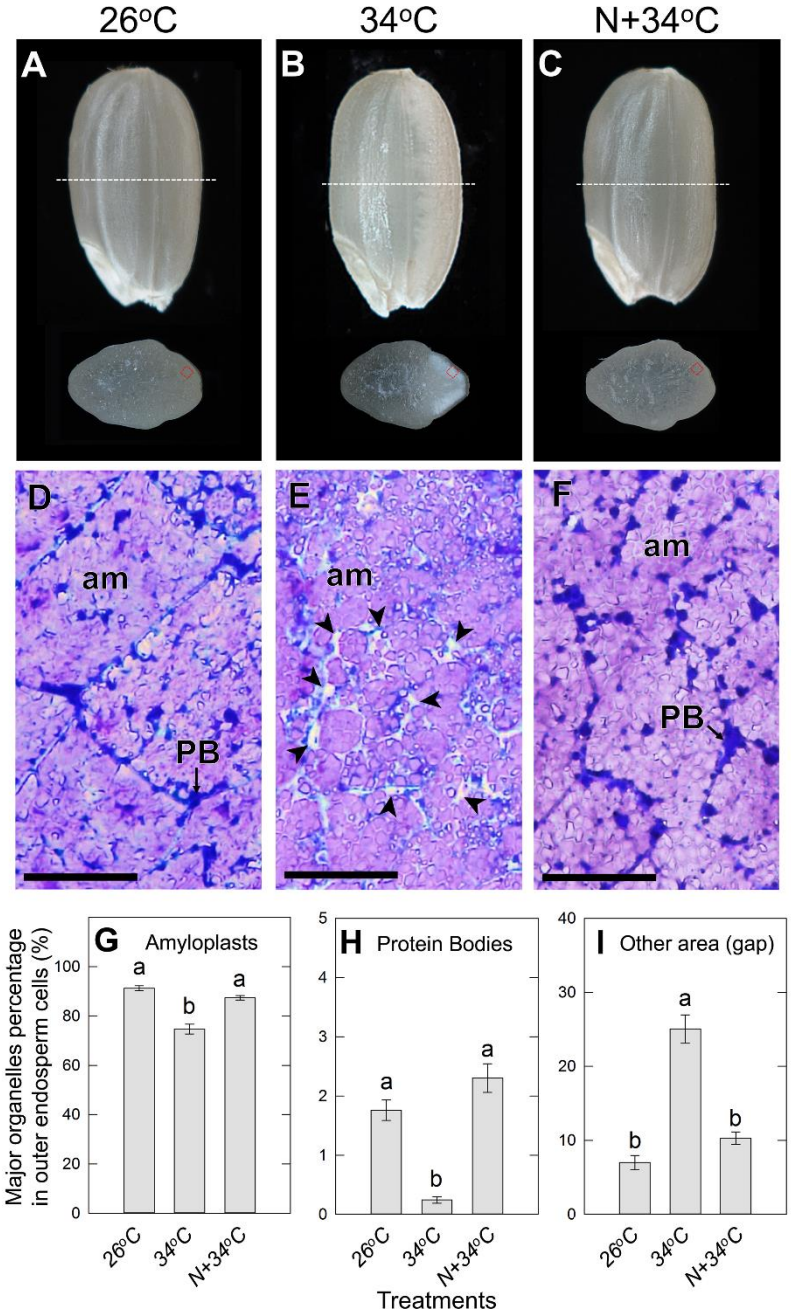

Figure 1. Images of rice kernel and the transverse sections of 26°C (A), 34°C (B), and N+34°C (C) treatments at maturation (40 DAH). Light microscopic images taken in the vicinity of the outer endosperm in the dorsal side of kernels harvested in 26°C (D), 34°C (E), and N+34°C (F) treatments, corresponding to the red dotted square on the transverse sections inserted in A-C. Grain sections of D-F were double-stained with Coomassie brilliant blue and iodine-potassium iodide. In D-E, PB, protein body; am, amyloplast. Arrows in E indicate gap areas. Bars in D-F indicate 50 μm. Area-based percentages of major organelles, amyloplasts (G), protein bodies (H), and other area (gap) (I) occupying in the outer endosperm cells in 26°C, 34°C, and N+34°C treatments were shown. The data indicate that the means±SE of 11-25 individual cells collected from at least 3 kernels from 3 individual plants in each treatment. Different letters in G-I indicate a significant difference (Tukey's HSD test, $p < 0.05$).

Figure 2

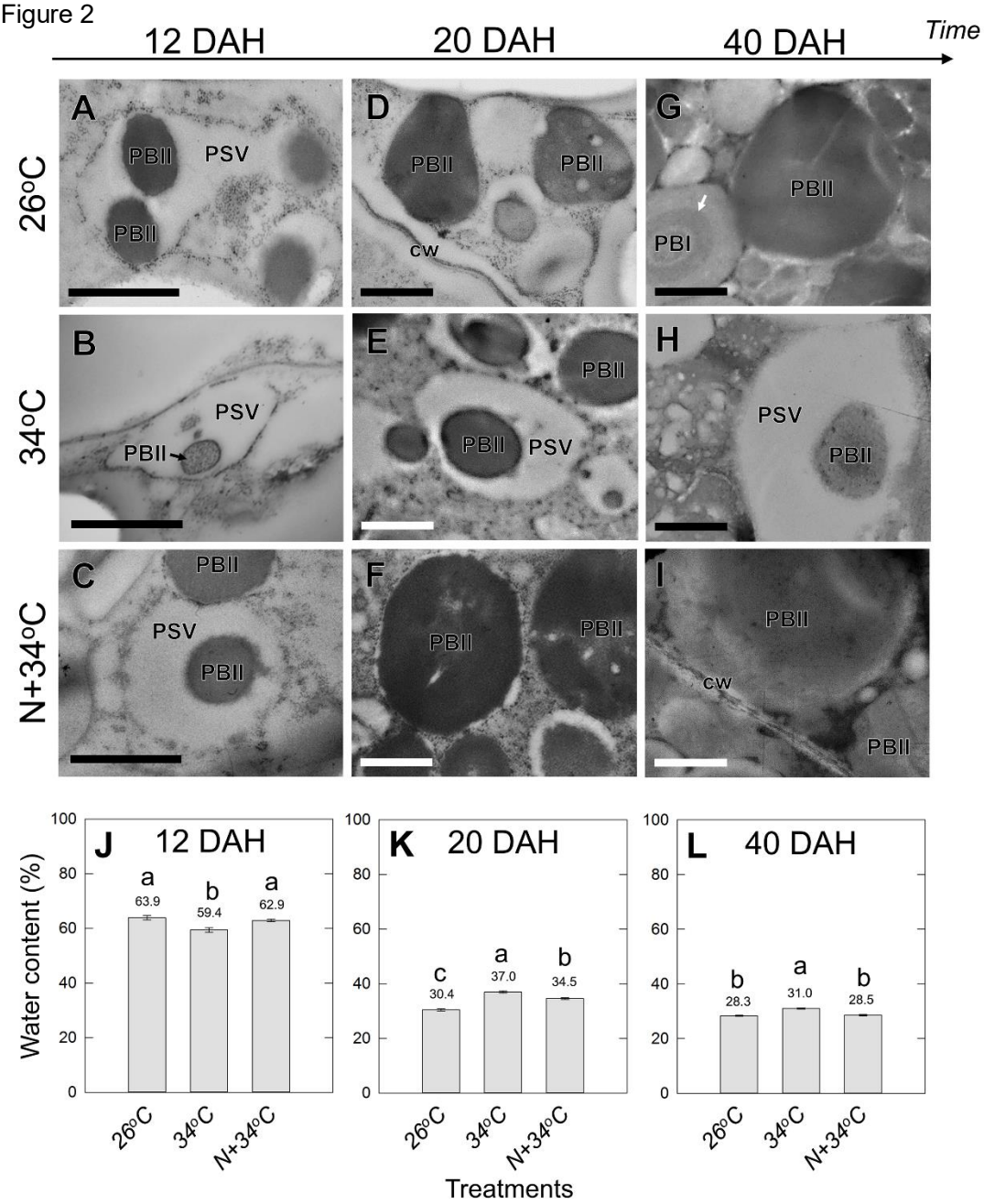

Figure 2. TEM images of the outer endosperm cells in 26°C (A, D, G), 34°C (B, E, H), and N+34°C (C, F, I) treatments collected at 12 (A-C), 20 (D-F), and 40 DAH (G-H). Water contents of rice grain kernels in each treatment at same three ripening stages are shown (J-L). Data are means±SEs of 18 kernels collected from 3 plants, and means are shown on the bars in each figure. Different letters indicate a significant difference among treatments (Tukey's HSD test, $p < 0.05$). In A-I, PSV, protein storage vacuole; PBI, protein body type I; PBII, protein body type II; cw, cell wall; rER, rough-surfaced endoplasmic reticulum. In G, each arrow indicates the deep-colored areas of Cys-rich 10-kDa layer formed in PBI. Bars indicate 1 μm.

Figure 3

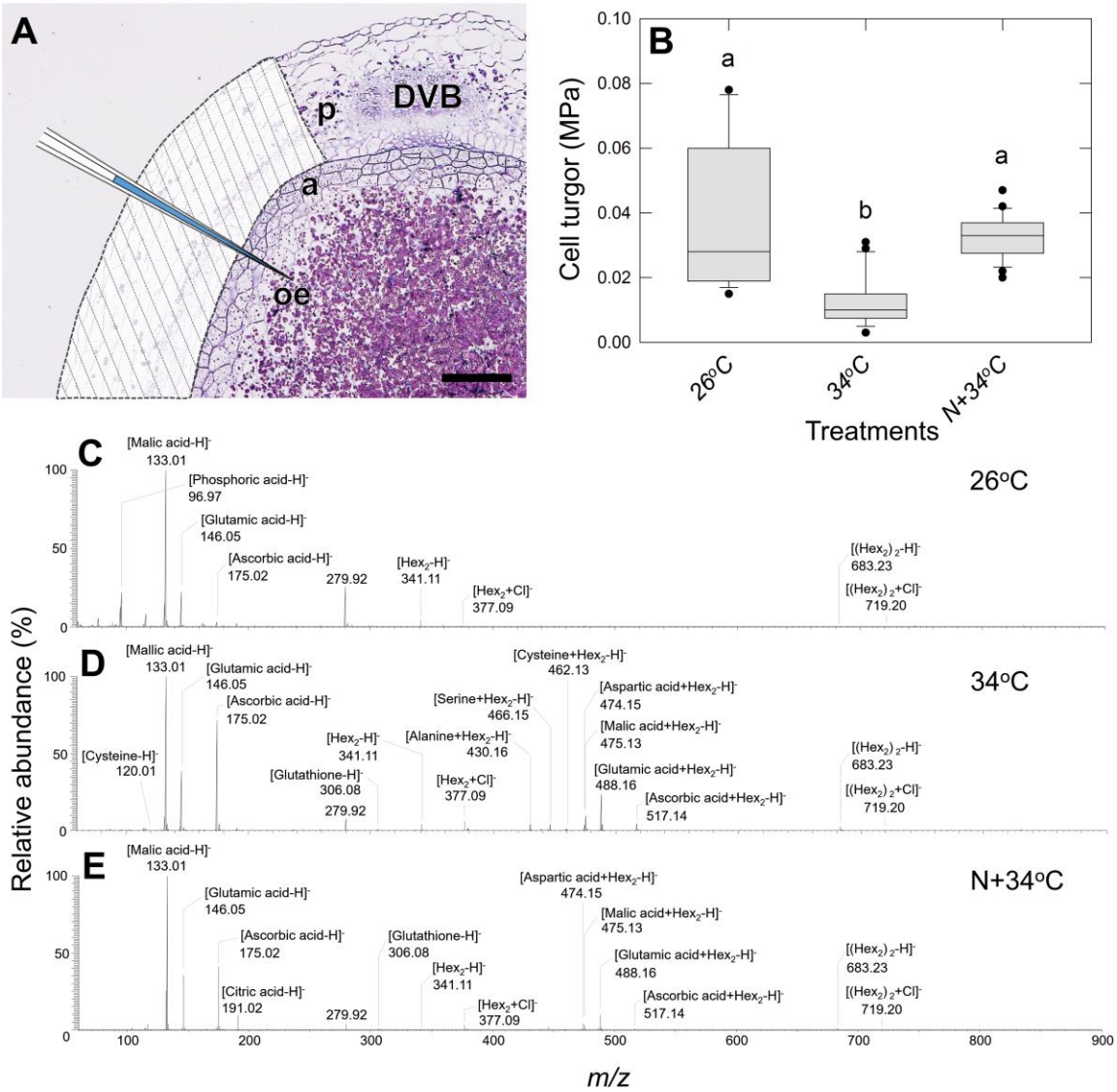

Figure 3. Image of the transverse section of the dorsal side of rice kernel at the early ripening stage (12 DAH) (A). In A, an image of cell sap extraction using a pressure probe from the outer endosperm cells was also drawn. A part of the pericarp shown in white with oblique lines was removed prior to the insertion of a probe tip, and a cell pressure probe was introduced (see Materials and Methods). DVB, dorsal vascular bundle; a, aleurone layer; oe, outer endosperm; p, pericarp. Bar indicates 100 μm. In B, box plot illustrating the variations of outer endosperm cell turgor in each treatment assayed at the same stage. Data are mean±SEs for 14-29 cells from 7-8 kernels from at least three different plants in each treatment. Different letters indicate a significant difference among treatments (Tukey's HSD test, $p < 0.05$). C-E, PicoPPESI-MS negative ion mode mass spectra obtained from the cells in 26°C (C), 34°C (D), and N+34°C (E) treatments at the same stage. Data are representative of similar experiments with 4-5 kernels in each treatment.

Figure 4

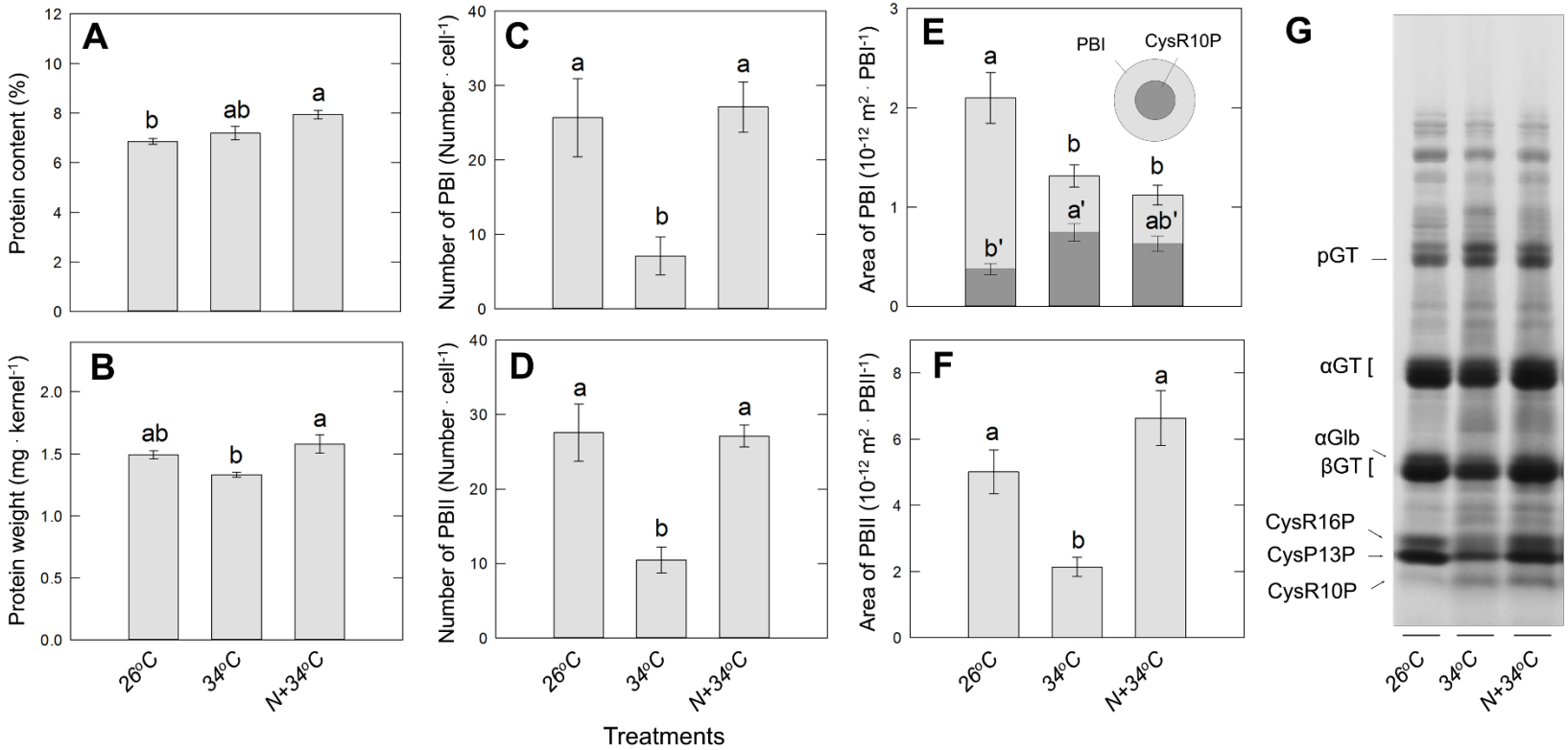

Figure 4. Protein content (A) and protein weight (B) of kernels in each treatment at 40 DAH. Data in A and B are mean±SEs for four plants. C-F, the number (C, D) and cross section area (E, F) of PBI (C, E) and PBII (D, F) in the outer endosperm cells morphometrically analyzed with the TEM images at 40 DAH (see Figure 2G, H, I). Each parameter in C-F indicates mean±SEs for 25-59 PBs from at least three kernels. In E, each deep-gray bar embedded in the light gray bars showing the area of PBI indicates the area of Cys-rich 10-kDa layer, which locates at the core of PBI (see inset). Different letters in A-F represents significant differences among treatments (Tukey's HSD test, $p < 0.05$) within the protein content, protein weight, and the area and number of both PBs (letter only) and area of Cys-10-kDa layer of PBI (’). In G, SDS-PAGE analysis of one-third of dorsal side of kernel, corresponding to the chalky zone in 34°C treatment. CysR10P, Cys-rich 10-kDa prolamin; CysR16P, Cys-rich 16-kDa prolamin; CysP13P, Cys-poor 13-kDa prolamin; pGT, proglutelins; αGT, glutelin acidic subunit; βGT, glutelin basic subunit; αGlb, α-globulin.

Figure 5

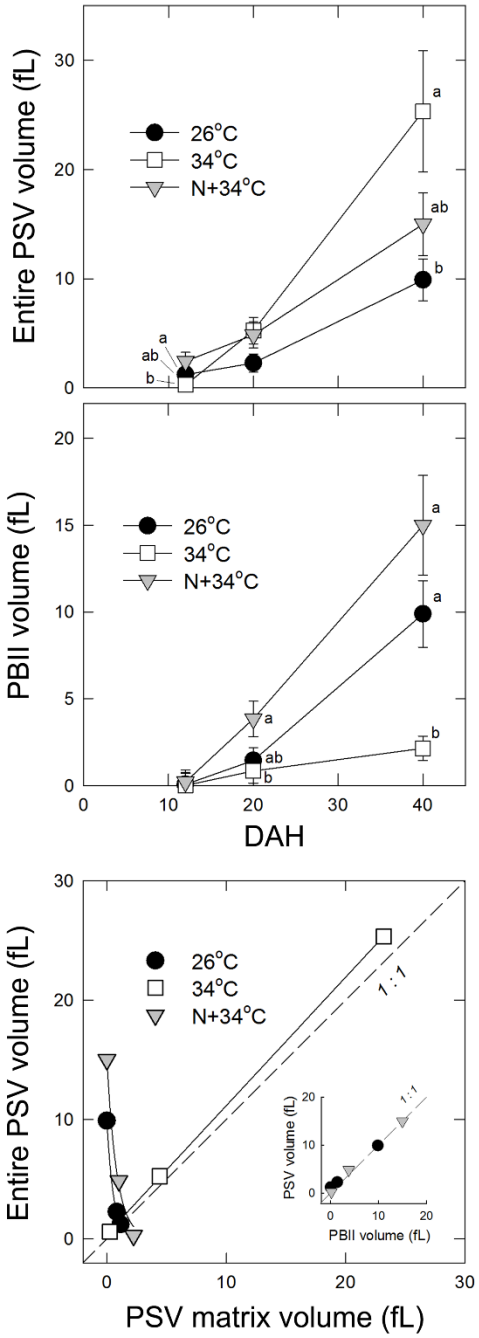

Figure 5. Time course of changes in the estimated PSV (A) and PBII (B) volumes in each treatment. In C, the PSV volume as a function of the corresponding PSV matrix volume. Closed circle, opened square, and gray downward-pointing triangle indicate 26°C, 34°C, and N+34°C treatments, respectively. Each point indicates mean±SEs calculated from areas of 4-38 PSVs or PBIIs. In A and B, nitrogen application at 4 DAH was shown, and the thick black bars at the x-axis indicate the duration of 34°C treatment. Different letters in A and B indicate significant differences among treatments (Tukey's HSD test, p <0.05). In C, the regression line between the PSV matrix volume (x) and the entire PSV volume (y) in 34°C treatment was $y = 1.08x + 0.41$ with $r^2 = 0.99$ ($p < 0.01$). Inset in C shows the relationship between PSV volume (y) and PBII volume (x) in 26°C and N+34°C treatments, and the regression lines in 26°C and N+34°C were y=0.89x with r^2=0.99 (p < 0.01) and y=0.98x+0.01 with r^2=0.99 (p<0.05), respectively. Each dashed line in C indicate a 1:1 line.

Figure 6

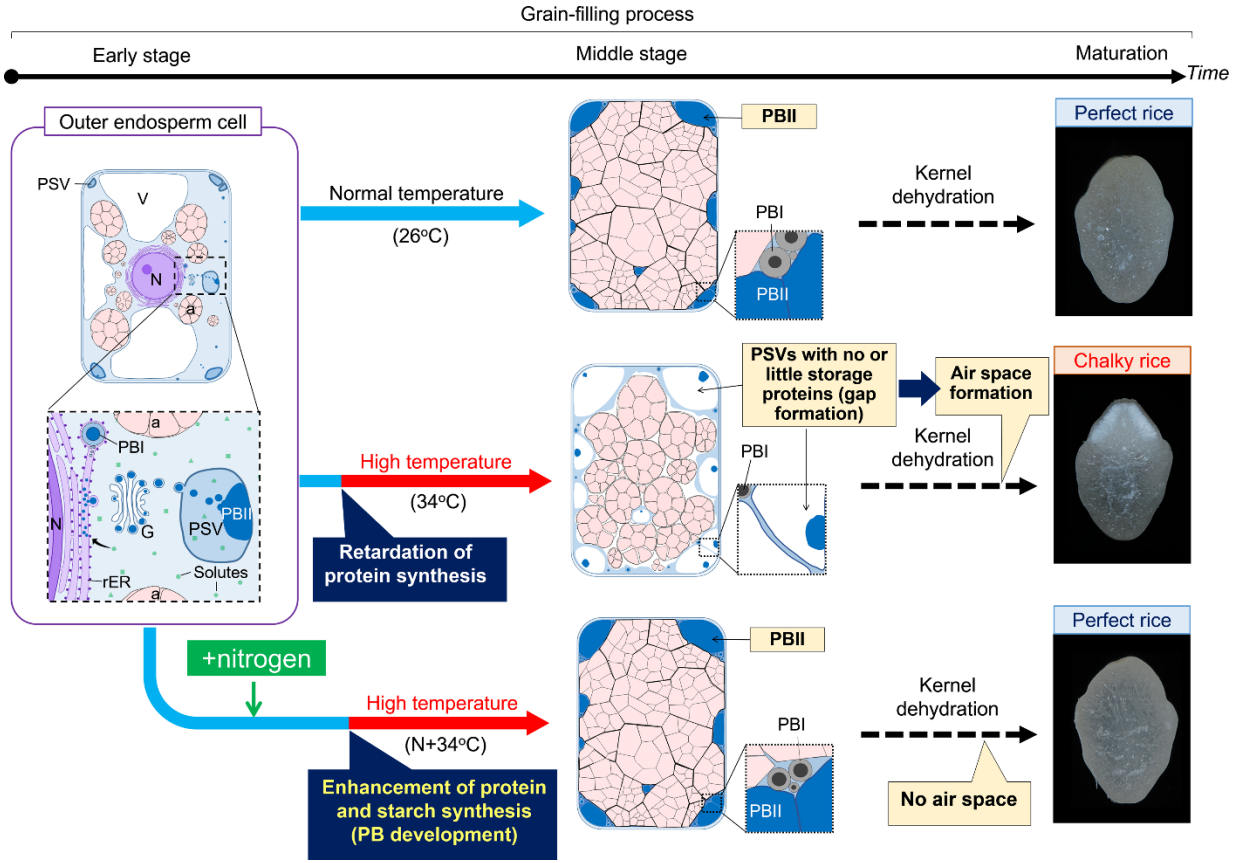

Figure 6. Schematic diagrams of the putative process of heat-induced chalky formation and nitrogen-enhanced adaptation in the dorsal outer endosperm cells. In the cells under normal conditions (26°C treatment), as the packing density of amyloplasts in the cells increases according to the reduction in the cytosol occupied with mainly vacuoles, resulting in the adequate development of amyloplasts and PBs to diminish cytosolic space (see Supplementary file 4C, F and I). When N level is low prior to high temperature (34°C treatment), the cells adjust less osmotically and reduce protein synthesis rate to preserve PSVs and vacuoles (see Discussion), resulting in air space formation during kernel dehydration, which turns to chalk. When N supply is adequate in the cells prior to high temperature (N+34°C treatment), cells sustain protein synthesis rate by strong osmotic adjustment to promote normal PB and amyloplast development, which diminishes cytosolic space, resulting in a substantial increase in perfect rice.